Dynamic activation of K_{ATP} channels in rhythmically active neurons

M. Haller, S. L. Mironov, A. Karschin* and D. W. Richter

*Physiologisches Institut, Georg August-Universität Göttingen, Humboldtallee 23, D-37073 Göttingen and *Max-Planck-Institut für biophysikalische Chemie, Am Faßberg 11, 37077 Göttingen, Germany*

(Received 20 April 2001; accepted after revision 5 July 2001)

1. The respiratory centre within the brainstem is one of the most active neuronal networks that generates ongoing rhythmic activity. Stabilization of such vital activity requires efficient processes for activity-correlated adjustment of neuronal excitability. Recent investigations have shown that a regulatory factor coupling electrical activity with cell metabolism comprises ATP-dependent K^+ channels (K_{ATP} channels), which continuously adjust the excitability of respiratory neurons during normoxia and increasingly during hypoxia.

2. We used the single-cell antisense RNA amplification-polymerase chain reaction (PCR) technique to demonstrate that respiratory neurons co-express the sulphonylurea receptor SUR1 with the Kir6.2 potassium channel protein.

3. Single channel measurements on rhythmically active inspiratory neurons of the brainstem slice preparation of newborn mice revealed that K_{ATP} channels are periodically activated in synchrony with each respiratory cycle.

4. The Na^+–K^+-ATPase was inhibited with ouabain to demonstrate that oscillations of the channel open probability disappear, although respiratory activity persists for a longer time. Such findings indicate that K_{ATP} channel open probability reflects activity-dependent fluctuations in the ATP concentration within submembrane domains.

5. We also examined the effects of extracellular $[K^+]$ and hypoxia. All changes in the respiratory rhythm (i.e. changes in cycle length and burst durations) affected the periodic fluctuations of K_{ATP} channel activity.

6. The data indicate that K_{ATP} channels continuously modulate central respiratory neurons and contribute to periodic adjustment of neuronal excitability. Such dynamic adjustment of channel activity operates over a high range of metabolic demands, starting below physiological conditions and extending into pathological situations of energy depletion.

K_{ATP} channels are hetero-octamers consisting of two different subunits, i.e. four inwardly rectifying K^+ channel subunits, either Kir6.1 or Kir6.2, and four sulphonylurea receptors (SUR), which belong to the family of ATP-binding cassette (ABC) transporters (Aguilar-Bryan & Bryan, 1999; Baukrowitz & Fakler, 2000). They are characterized by strong inhibition by intracellular ATP and activation by MgADP. Such ATP/ADP dependence of K_{ATP} channels enables a metabolic control of neuronal excitability. Besides ATP/ADP ratios, K_{ATP} channel activity is also modulated by various intra- and extracellular factors such as low pH, adenosine, various G protein-coupled processes and the cytoskeleton (Cason *et al.* 1995; Hilgemann, 1997; Hiraoka, 1997; Aguilar-Bryan & Bryan, 1999; Baukrowitz & Fakler, 2000).

K_{ATP} channels are incorporated in several tissues including smooth muscle, cardiac myocytes, skeletal muscle and pancreatic β-cells. In the brain, K_{ATP} channels were reported in neurons of the hippocampus (Zawar *et al.* 1999), cortex (Jiang & Haddad, 1997) and the brainstem (Pierrefiche *et al.* 1996; Karschin *et al.* 1998). The functional significance of K_{ATP} channels is best described for the pancreas and the heart. In the pancreas, K_{ATP} channels act as a major regulator of insulin secretion, hyperglycaemia leading to an increase in ATP, which closes K_{ATP} channels, thereby causing membrane depolarization, Ca^{2+} influx and stimulation of insulin secretion (Miki *et al.* 1998). In cardiac cells, a fall of ATP levels during metabolic impairment activates K_{ATP} channels and thus modulates cardiac contractions (Terzic *et al.* 1995). Both pancreatic β-cells (Larsson *et al.* 1996)

and cardiomyocytes (O'Rourke *et al.* 1994) revealed oscillatory variations of K_{ATP} conductances ($g_{K_{ATP}}$), which were attributed to oscillations in the glycolytic pathway (Prentki *et al.* 1997). In the pancreas, periodic activation of $g_{K_{ATP}}$ was reported to cause oscillations of electrical activity and $[Ca^{2+}]_i$ fluctuations during glucose stimulation (Larsson *et al.* 1996; Kinard *et al.* 1999). A similar rhythmic behaviour was observed in cardiomyocytes (O'Rourke *et al.* 1994), where metabolic stress initiates cyclic activation of K_{ATP} channels and suppression of depolarization-evoked $[Ca^{2+}]_i$ transients.

Studies on the functional significance of $g_{K_{ATP}}$ in the brain have focused mostly on its contribution to hypoxic responses of neurons. Here we describe for the first time oscillatory activation of neuronal K_{ATP} channels in synchrony with normal rhythmic neuronal activity. Our test model is the respiratory network, which generates a very robust rhythm of alternating burst activities. The rhythm originates from a morphologically well-defined region located in the lower brainstem – the pre-Bötzinger complex (Smith *et al.* 1991). This respiratory centre can be *in vitro* isolated in a rhythmic slice preparation to directly investigate respiratory neurons for periodic modulation of excitability through K_{ATP} channels. Respiratory neurons are adequate models, because they receive periodic inhibitory and excitatory inputs that induce spontaneous, 1–2 s long-lasting bursts of action potentials every 3–4 s. Such intense burst discharges induce significant changes in transcellular ion concentrations, which demand high metabolic efforts for restoration. K_{ATP} channels are expected to be involved in this regulation.

Previously, we have analysed single K_{ATP} channels in respiratory neurons, determined a conductance of 75 pS and verified effective blockade by increased $[ATP]_i$, glibenclamide or tolbutamide and modulation by adenosine, diazoxide and hypoxia (Mironov *et al.* 1998). Blockade of K_{ATP} channels was observed to induce membrane depolarization and increase of neuronal excitability (Pierrefiche *et al.* 1996).

In this study, we analysed the molecular structure of the channel using the single-cell antisense RNA amplification-polymerase chain reaction (PCR) technique and determined the fluctuations of K_{ATP} channel activity during ongoing respiratory activity. We also tested for the effects of the Na^+–K^+ pump blocker ouabain, changes in the extracellular potassium concentration ($[K^+]_o$) and hypoxic stimuli. Such measurements indicate a Na^+–K^+ pump-correlated mechanism for such oscillations.

METHODS

Slice preparation

Experiments were performed on a medullary slice preparation from neonatal NMRI mice (P5–P8) containing the kernel of the respiratory centre, which is spontaneously active (Smith *et al.* 1991). The technique of tissue isolation followed the approach developed for mice (Mironov *et al.* 1998). All animals were housed, cared for and killed in accordance with the recommendations of the European Commission (no. L358, ISSN 0378-6978), and protocols were approved by the Committee for Animal Research, Göttingen University.

The brainstem–spinal cord was isolated in ice-cold artificial cerebrospinal fluid (ACSF) and a single 700 μm thick transverse slice containing the pre-Bötzinger complex was cut from the brainstem, transferred to the recording chamber and mounted on the stage of an upright microscope (Axioscope, Zeiss, Oberkochen, Germany). The slice was fully submerged in continuously flowing ACSF (28 °C, 40–50 ml min^{-1}) that was gassed with carbogen (95% O_2 and 5% CO_2). The perfusing solution was pumped to the experimental chamber through stainless-steel tubing to prevent leakage of dissolved gases. The ACSF solution was composed of (mM): 128 NaCl, 3 KCl, 1.5 $CaCl_2$, 1.0 $MgSO_4$, 21 $NaHCO_3$, 0.5 NaH_2PO_4 and 30 D-glucose. Solutions of various K^+ concentrations were obtained by replacing NaCl with KCl. The respiratory rhythm was recorded with suction electrodes from a rootlet of the hypoglossal nerve.

All drugs were applied directly to the bath and arrived at the experimental chamber after a delay of 8–12 s. Recovery was obtained by perfusing 400–500 ml fresh ACSF solution. Distinct activity levels of the respiratory network were attained by varying $[K^+]_o$ levels between 3 and 12 mM. In order to induce hypoxic conditions, bath gases were changed from carbogen to 95% N_2 and 5% CO_2. Tissue oxygen pressure (P_{O_2}) was measured occasionally with oxygen-sensitive electrodes (Diamond Electro-Tech Inc., Ann Arbor, MI, USA) as described previously (Ballanyi *et al.* 1996; Mironov *et al.* 1998). A P_{O_2} electrode was placed 100 ± 25 μm below the slice surface into the region where respiratory neurons were located. Fifteen to twenty seconds after O_2 was replaced by N_2 in the bath solution, extracellular tissue P_{O_2} fell from 232 ± 39 to 6 ± 4 mmHg and remained constant ($n = 15$, $P < 0.05$) thereafter.

Electrophysiological recordings

Patch electrodes were manufactured from borosilicate glass (Clarke Electromedical, Pangbourne, UK), had tip openings of 1–2 μm and a DC resistance of 2–4 MΩ. Signals were fed to an EPC-7 patch-clamp amplifier (ESF, Friedland, Germany). Cells were either patched under visual control or 'blindly'. Electrodes with an imposed internal hyperbaric pressure of 10–30 mmHg were inserted into tissue with a micromanipulator (Eppendorf-Netheler-Hinz GmbH, Hamburg, Germany) and slowly advanced through the tissue until an increase in pipette series resistance indicated contact with a cell. Following the formation of a gigaseal, channel activity and spike discharges were recorded in the cell-attached mode (usually with an applied potential of +40 mV that corresponds to a membrane potential of −100 mV, assuming a resting potential of −60 mV). K_{ATP} channels were identified by their conductance and gating characteristics as detailed previously (Mironov *et al.* 1998). Channel identity was verified by application of specific K_{ATP} channel blockers (glibenclamide, tolbutamide) or activators (diazoxide).

Hypoglossal (XII) rootlets were recorded with a blunt suction electrode to monitor the central respiratory rhythm. XII activity was amplified 5000–10 000 times, bandpass filtered (0.25–1.5 kHz), rectified and integrated (Paynter filter with a time constant of 50–100 ms).

All recordings were stored on a MacLab acquisition system (WissTech GmbH, Spechbach, Germany) for off-line analysis.

Data analysis

Defined periods of cell-attached channel recordings of 3 s duration containing inspiratory bursts were exported for analysis to Igor Pro (WaveMetrics, Inc., Lake Oswego, USA). Cell-attached recordings

from inspiratory neurons displayed capacitive responses to action potential (AP) discharges (Lynch & Barry, 1989; Rajendra *et al.* 1992). The number of these APs ranged between 3 and 15 per inspiratory burst. In order to avoid interference with the recordings of channel activity, AP discharges were removed. Each AP was replaced by the mean level of channel activity averaged over 5 ms before and after the AP. K_{ATP} channel openings occurring simultaneously with AP discharge were thus deleted and the open probability was probably slightly underestimated during the periods of respiratory bursts. However, it is important to note that such a subtraction protocol did not significantly change or induce oscillations of channel open probability (see Discussion). Following the removal of APs the channel activity was isolated by setting the background noise (± 5 pA) to baseline levels.

The open probability (P_o) of K_{ATP} channels was determined by dividing the mean of channel currents collected during up to 200 traces, by unitary current amplitudes and the number of identifiable channels. Finally the traces were smoothed with a 'box-smoothing algorithm'.

Statistica software (StatSoft GmbH, Tulsa, USA) was used to assess the statistical significance ($P < 0.05$) of fluctuation parameters based on the Mann-Whitney U test.

Molecular biology

In order to harvest cytosol for RT-PCR analysis, cells were patched and identified as inspiratory neurons in the cell-attached configuration. After the whole-cell configuration was established, constant suction was applied for 1–2 min to aspirate the cytoplasm, while the access resistance was monitored to verify persistence of gigasealing. Amplification of the antisense RNA (aRNA) from single respiratory neurons was performed according to the procedure described in detail by Eberwine *et al.* (1992). In brief, 2.5 mM dideoxynucleotides (dNTPs), 2 ng μl^{-1} T7-oligo-d(T)24 primer and 0.5 U μl^{-1} avian myeloblastosis virus (AMV) reverse transcriptase (Roche Diagnostics, Mannheim, Germany) were mixed with the cytosol and incubated for 60–90 min at 37 °C for reverse transcription. Second-strand synthesis was performed with T4 DNA polymerase and Klenow fragment (1 U μl^{-1} each) followed by treatment with S1 nuclease (1 U μl^{-1}) and subsequently Klenow enzyme (1 U μl^{-1}) to remove hairpin loops and to produce blunt ends of the cDNA. After aRNA amplification with 100 U μl^{-1} T7 RNA polymerase, a second amplification, including the final synthesis of double-stranded cDNA, was conducted to yield adequate amounts of template for the expression profiling of different mRNAs from a single respiratory neuron. All amplification steps were conducted under RNase-free conditions. In the mouse both SUR1 and SUR2 genes contain multiple introns, but the Kir6 isoforms are intronless. To exclude contaminations by genomic DNA, control experiments were performed without AMV reverse transcriptase, or amplified aRNA was incubated after each amplification with RNase-free DNase I at 37 °C for 1 h. Polymerase chain reaction analysis was performed using as template (i) 1/50 of the total volume of the final aRNA amplification product, and (ii) alternatively, mRNA from single neurons that had been reverse transcribed for 60 min using 2.5 mM dNTPs, 25 μM random hexamer primers, 10 mM dithiothreitol, 2 U μl^{-1} RNase inhibitor and 10 U μl^{-1} M-MuLV reverse transcriptase (Roche Diagnistics). Kir6 and SUR core fragments were amplified with primers based on the cDNA sequences of Kir6.1 (Yamada *et al.* 1997), Kir6.2 (Sakura *et al.* 1995), SUR1 (Aguilar-Bryan *et al.* 1995) and SUR2 (Isomoto *et al.* 1996). Sense and antisense primers were chosen to specifically amplify fragments of 539–865 bp in length: mKir6.1 (Genbank accession number D88159, 865 bp), sense primer 5′-GAAGATGCTGGCCAGGAAGAG-3′, antisense primer 5′-CAGCCACTGACCTTGTCAACC-3′; mKir6.2 (MMU73626; 553 bp), sense primer 5′-GGAGAGGAGGGCCCG-CTTCGTGTC-3′, antisense primer 5′-GGCGCTAATGATCATGC-TTTTTCGGAGGTC-3′; rSUR1 (L40624, 539 bp), sense primer 5′-GCAGCCGAGAGCGAGGAAGATGA-3′, antisense primer 5′-ACA-GCCAGGGCGGAGACACAGAGTA-3′; mSUR2 (D86037, 603 bp), sense primer 5′-CGCGGCGGTCATCGTGCTC-3′, antisense primer 5′-CGCCGCGCCTGCTCGTAGTT-3′ (conserved for SUR2A and SUR2B).

PCR amplifications were run with *Taq* polymerase (Qiagen, Hilden, Germany) for 35 cycles at 95 °C denaturing, 52–58 °C annealing, and 72 °C extension for 1.5 min each, with a final extension of 15 min at 72 °C. Amplified fragments were purified from agarose gels, digested at terminal restriction sites or blunt ends produced, and ligated into pBluescriptSKII vector (Stratagene, La Jolla, CA, USA). Double-stranded sequencing of the PCR products was performed on both strands using the Prism Sequenase dye terminator kit on an automatic sequencer (Perkin Elmer, Weiterstadt, Germany).

All Kir6 and SUR primers were tested for functionality and sensitivity with 0.05–0.1 ng of original cloned cDNA as template (and 50 ng of mouse tissue DNA). Amplified fragments of the neurofilament middle protein (NF-M) confirmed that the cytosol had been aspirated from neurons and not from glial cells. Moreover, adequate H_2O controls performed for all primer combinations were negative.

RESULTS

Molecular biology of the K_{ATP} channel

For identification of the molecular composition of K_{ATP} channels, the harvested cytosol was processed either for aRNA/cDNA amplification ($n = 2$) or directly reverse-transcribed for subsequent PCR analysis ($n = 4$). Figure 1 shows the Kir6/SUR expression profiling after aRNA processing for two inspiratory neurons. The primer pair that was designed to amplify a Kir6.1 fragment revealed a strong 865 bp band from the vector template, but not from the cDNAs of the single respiratory neurons (using 1/50 of the total aRNA amplification product). Likewise, the primer combination that successfully amplified a 603 bp SUR2 fragment from atrial cDNA (50 ng) failed to produce detectable amplification products from the single cell source. In contrast, clearly detectable fragments were observed using Kir6.2 (552 bp) and SUR1 (539 bp) primers with cDNA from the two nerve cells. The same expression pattern, i.e. strong expression of Kir6.2/SUR1 and absence of Kir6.1/SUR2 signals, was detected in all four inspiratory neurons directly processed for RT-PCR after recording. When subcloned, grown to a large scale and sequenced on both strands, the amplified fragments were always identical to the published cDNA sequences. Thus PCR analysis of unprocessed and T7 RNApolymerase-amplified RNA with specific primers revealed that SUR1 and Kir6.2 isoforms translate to form the major subtype of K_{ATP} channel in inspiratory neurons.

Functional modulation of ongoing K_{ATP} channel activity

Normoxic activities of respiratory neurons are effectively modulated by K_{ATP} channels (Pierrefiche *et al.* 1996). This was verified by the changes of ongoing respiratory activity after application of the K_{ATP} channel blockers

glibenclamide (30–50 μM, $n = 4$) and tolbutamide (300–500 μM, $n = 6$). As shown in Fig. 2*A* such blockade of K_{ATP} channels resulted in an increase of the amplitude of integrated hypoglossal (XII) bursts of 9.6 ± 7.1 % (mean ± S.D., $n = 7$). The frequency of bursts was not affected. The changes of hypoglossal bursts corresponded with an increase in the amplitude of synaptic drives by 4.9 ± 2.7 % (mean ± S.D., $n = 4$) in individual respiratory neurons (Fig. 2*B*).

Because of ongoing rhythmic bursting of respiratory neurons, we analysed whether channel activity also varies periodically. Figure 3*A* shows recordings from a neuron that was identified as inspiratory because of its discharge in synchrony with inspiratory hypoglossal (XII) activity. A time window of 3 s covering the duration of the inspiratory burst is depicted in Fig. 3*B*. Hypoglossal burst activity and the underlying grey area indicate the timing of inspiration. The trace below (grey)

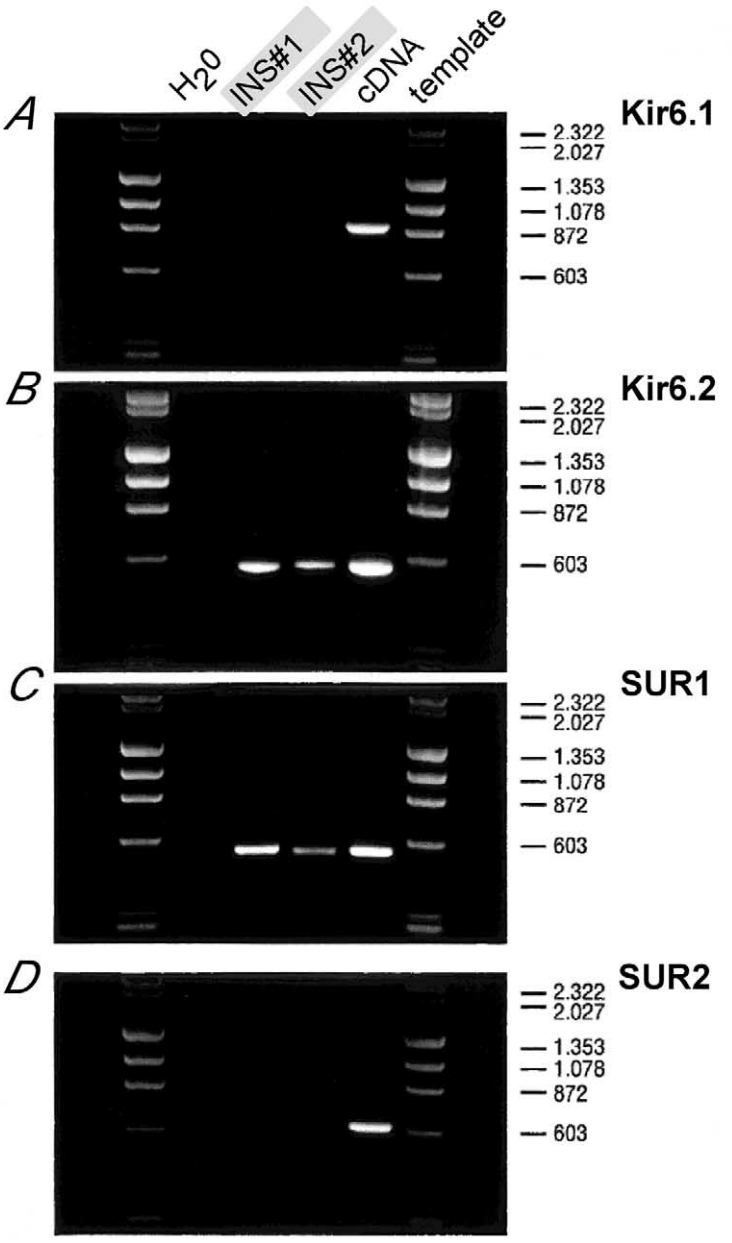

Figure 1. PCR analysis of amplified aRNA from single respiratory brainstem neurons

DNA fragments are amplified with primer pairs specific to Kir6.1 (*A*), Kir6.2 (*B*), SUR1 (*C*) and SUR2 (*D*). The first lanes next to the molecular weight marker (λHindIII-ΦXHaeIII digest) are H_2O controls, templates in lanes 2 and 3 were of two different inspiratory neurons (INS#1, INS#2), and lane 4 used 0.1 ng of plasmid cDNA as positive control (except in *D* where 50 ng of atrial cDNA was used). Primers were sensitivity-tested to amplify fragments of 865 bp (Kir6.1), 553 bp (Kir6.2), 539 bp (SUR1) and 603 bp (SUR2). Fragment sizes of the molecular marker are indicated on the right. Note that fragments amplified from single respiratory neurons can only be detected for Kir6.2 and SUR1.

shows a sample of cell-attached recordings (I_m). In order to selectively isolate channel activities, we eliminated action potentials and background noise (see Methods), as indicated by a superimposed black trace. A whole-cell recording – obtained after 'breaking into' the cell – indicates the timing of the synaptic drive.

An accurate estimate of channel open probability (P_o) was then obtained by averaging 200 cell-attached traces and treating this average with a box-smoothing algorithm. Direct comparison of P_o fluctuations is complicated by the large variations between the open probabilities of individual cells. Thus in addition to the open probability (P_o), P_o changes were computed as $\Delta P_o/P_{min} \times 100$ (%) (Fig. 3*B*, lowest trace). The pattern of P_o fluctuations was consistent for all inspiratory neurons analysed ($n = 13$ cells). Such analyses revealed that P_o rises throughout inspiration to attain maximal levels at the end or shortly after the inspiratory burst and then declines to minimal levels before the onset of the next inspiratory phase.

A similar procedure of data acquisition performed for separate time windows set *before* (Fig. 3*C*, upper panel) and *after* (Fig. 3*C*, lower panel) inspiratory bursts resulted in similar fluctuations. Due to the spontaneous variations of cycle lengths, successive bursts sometimes fell into the same time frame as indicated by the second grey area.

Quantitative description of P_o modulations

The rise and fall of P_o did not follow single exponential functions, and therefore were defined by the parameters cycle time (T_{tot}), rise time 10–90 % ($t_{10–90\%}$), decay time 90–10 % ($t_{90–10\%}$), and the delay between onset of XII peaks and the 10 % point of P_o peaks (t_{delay}) (Fig. 4*A*). In addition, maximal P_o fluctuations ($\Delta P_{peak}/P_{min}$), were computed as peak-to-peak amplitudes divided by the minimum value of P_o.

Mean values (± S.E.M.) of these parameters obtained under control conditions, hypoxia, low $[K^+]_o$ and ouabain application are depicted in Fig. 4*B*. Statistically significant effects (Mann-Whitney U test, $P < 0.05$) were observed for T_{tot} (hypoxia, low $[K^+]_o$), $t_{10–90\%}$ (hypoxia, ouabain), $t_{90–10\%}$ (low $[K^+]_o$, ouabain) and $\Delta P_{peak}/P_{min}$ (ouabain). An average t_{delay} of 0.08 ± 0.12 s revealed that P_o fluctuations display relatively fast kinetics, allowing quick reactivity to each respiratory burst. This delay time did not change significantly with varying P_{O_2}, $[K^+]_o$ or ouabain application.

In order to verify activity-correlated fluctuation of P_o, we also analysed spontaneously active K_{ATP} channels in neurons that were either tonically active or silent (Fig. 5*B* and *C*, respectively). Such comparison showed that only inspiratory neurons exhibited distinct fluctuations with a mean $\Delta P_{peak}/P_{min}$ value of 85 ± 14 % (see Fig. 4*B*). In the other neurons, P_o fluctuations were absent or exhibited incomparably small amplitudes (< 10 %).

$[K^+]_o$-induced variation of cycle length

The respiratory rhythm can be changed by activating the respiratory network through elevation of $[K^+]_o$ (Smith *et al.* 1991). Figure 6*A* shows traces of hypoglossal recordings, P_o and $\Delta P_o/P_{min}$ fluctuations for elevated $[K^+]_o$

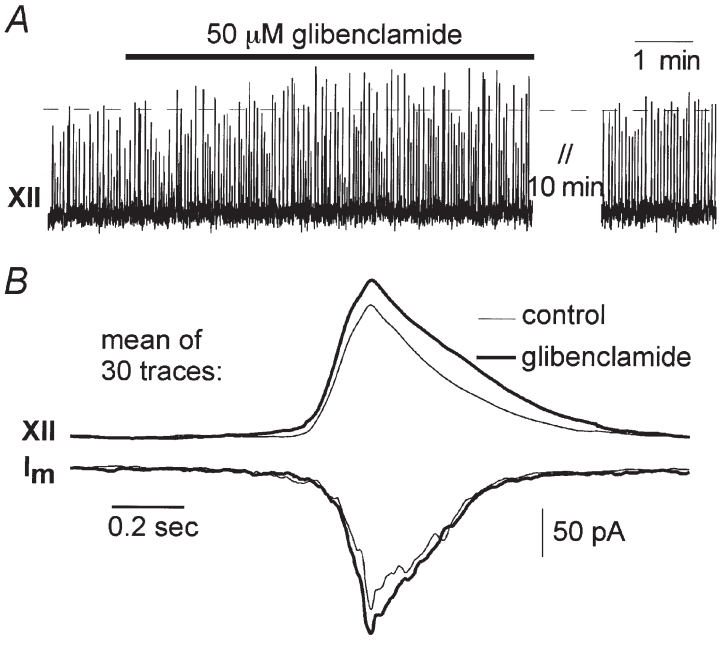

Figure 2. Respiratory rhythm and synaptic drive amplitude after glibenclamide application

A, the amplitude of the integrated hypoglossal nerve (XII) activity increases after glibenclamide application. *B*, modulation of synaptic drives (membrane currents, I_m, recorded in whole-cell mode at holding potential −60 mV) could only be discerned when 30 traces were averaged and smoothed. Synaptic drive amplitude increased with glibenclamide in parallel with hypoglossal activity.

of 8 or 11 mM. Under control conditions the respiratory rhythm was stabilized at high $[K^+]_o$ values of 9–11 mM. When P_o fluctuations during controls (13 cells) were compared with traces taken at lower $[K^+]_o$ (7–9 mM, 7 cells), the most sensitive parameter was $t_{90-10\%}$, which rose from 0.87 ± 0.11 to 2.04 ± 0.34 s, but T_{tot} also increased significantly (Fig. 4*B*), although the number of APs per burst did not change significantly when $[K^+]_o$ was varied. The maximal fluctuation, $\Delta P_{peak}/P_{min}$, decreased from $85 \pm 14\%$ (control) to $61 \pm 9\%$ ($[K^+]_o = 7$–9 mM). As the respiratory network was activated by increased levels of $[K^+]_o$, the cycle length shortened and the averaged P_o value increased. A plot of mean P_o values against cycle length is shown in Fig. 6*B*. Each point

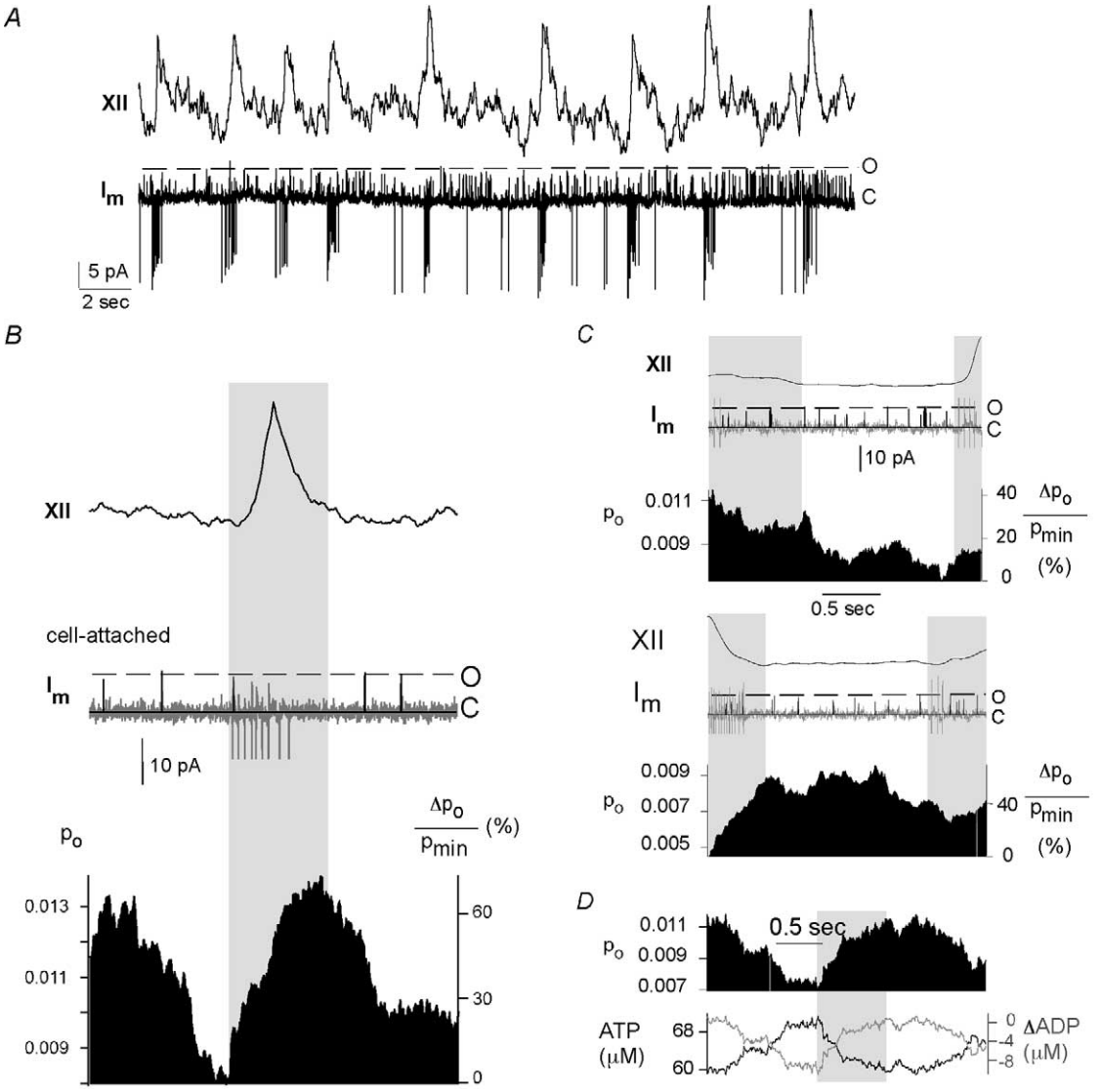

Figure 3. Modulation of K_{ATP} channel activity during a respiratory cycle

A, neurons were first identified as inspiratory by recording the bursting activity in the cell-attached mode with a pipette potential of +40 mV and correlating the membrane current, I_m, with the integrated hypoglossal rootlet activity (XII). *B*, a time window selected around a respiratory burst, which is marked by the grey area. The integrated hypoglossal activity (XII) as averaged over 200 traces is depicted on top. The traces below show samples of cell-attached recordings exhibiting single-channel openings as well as whole-cell recordings (voltage clamp) from the same cell. Action potential discharges and background noise were removed from the cell-attached measurements as described in the text, yielding the superimposed black trace. Displayed below is the open probability (P_o), obtained by averaging 200 such traces and smoothing with a box procedure. Also depicted is the relative change in P_o given by $\Delta P_o/P_{min} \times 100$ (%), where P_{min} is the minimum value of P_o. Alternatively, time windows were selected to contain the time period before (*C*, top panel) and after (*C*, bottom panel) the respiratory burst. *D*, $[ATP]_i$ values (lower panel) were estimated from P_o ($[ATP]_i = K_d(1/P_o^{1/4} - 1)$) with $K_d = 29\ \mu$M (Ashcroft & Gribble, 1998) for a sample P_o trace. Changes in ADP concentration were derived from $[ATP]_i$, assuming that all ATP is converted to ADP.

represents the mean (± S.E.M.) of ten cycles of similar duration. Linear regression revealed on average a slope of $-0.0012 \pm 0.0011\ s^{-1}$ for ten cells with a negative correlation coefficient of $r = -0.83$ ($P < 0.01$).

Effect of hypoxia on K_{ATP} channel modulation

Ongoing rhythmic activity requires a high energy turnover in respiratory neurons, and a functional way to manipulate energy supply is hypoxia. Figure 7*A* shows the hypoxic response in the hypoglossal nerve consisting of an initial augmentation with an increase in respiratory burst frequency that is followed by a secondary depression with a decline in burst frequency. Likewise, the amplitudes of respiratory bursts rose initially and then fell with a similar time course. Besides enhancement of respiratory activity, XII activity developed a characteristic tonic activation (Haddad & Donnelly, 1990). The effect of hypoxia on K_{ATP} channel P_o fluctuations was analysed during the period shortly before onset of hypoxic depression (indicated by the light grey area in Fig. 7*B*). Quantitative analyses of P_o could not be performed during later periods because of the low number of inspiratory bursts.

Figure 7*B* shows P_o and $\Delta P_o/P_{min}$ for traces obtained under control conditions (left panel, $n = 34$) as well as during hypoxic augmentation (right panel, $n = 21$). The duration of respiratory bursts is shown by the grey areas. Hypoxia led to a decrease in respiratory cycle length, T_{tot}, and an increase in P_o fluctuation, $\Delta P_{peak}/P_{min}$, to 109 ± 37 % (Fig. 4*B*). Also, the value for $t_{10–90\%}$ rose significantly in parallel with the hypoxic augmentation of AP discharge, which increases on average from 3.9 to 12.8 APs per burst (8 cells). As previously reported (Mironov *et al.* 1998), the

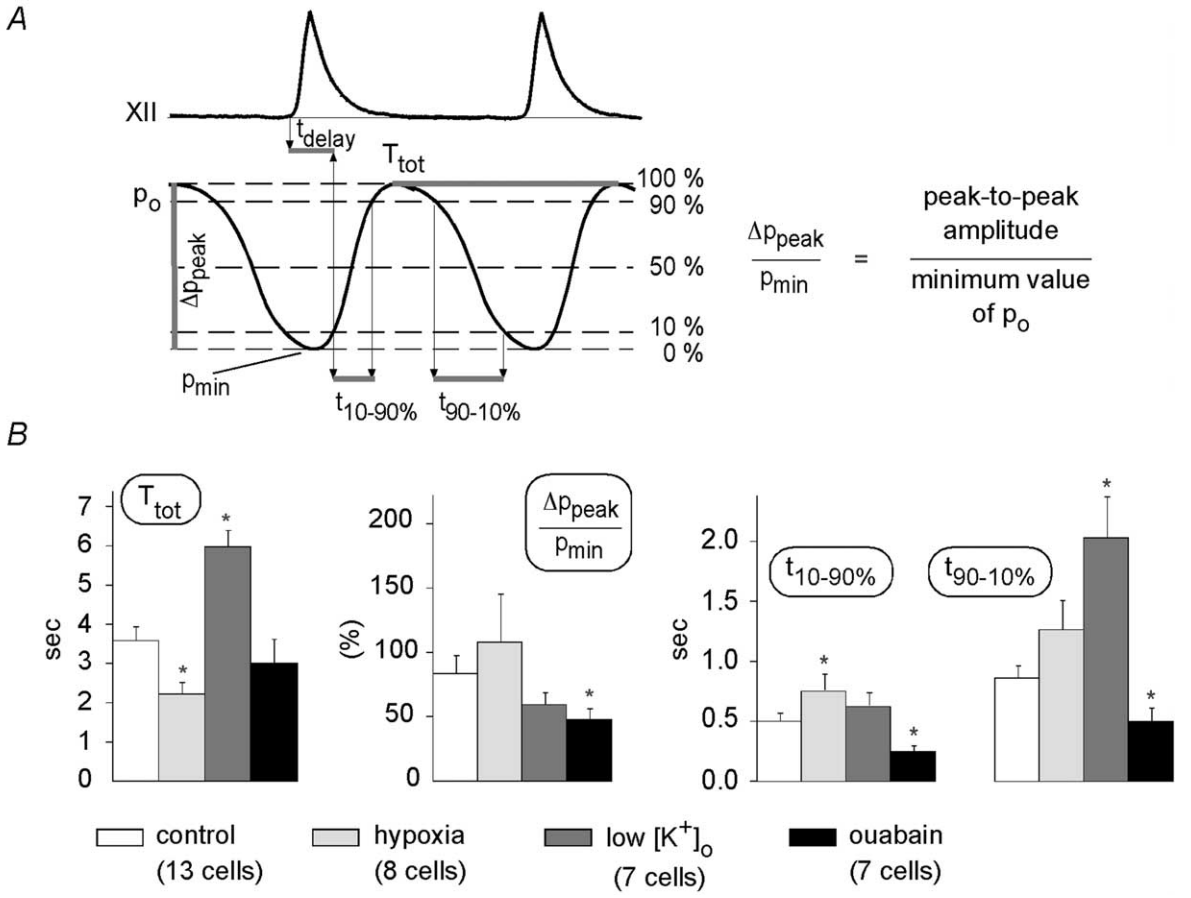

Figure 4. Parameters of P_o fluctuations

A, for a quantitative description of the changes in P_o fluctuations, the following parameters were analysed: t_{delay}, the delay between onset of the rise of hypoglossal nerve activity and the 10 % point of P_o; T_{tot}, the total duration of respiratory cycle; $t_{10–90\%}$, the rise time from 10 to 90 % of peak amplitude; $t_{90–10\%}$, the decay time from 90 to 10 % of peak amplitude; and $\Delta P_{peak}/P_{min}$, the maximum amplitude of P_o fluctuations, which is always given as the percentage increase in P_o. *B*, parameter (± S.E.M.) values were (at control conditions, hypoxia, low $[K^+]_o$ and after ouabain application, respectively): T_{tot} 3.61 ± 0.33, 2.24 ± 0.28, 6.00 ± 0.40, 3.04 ± 0.59; $t_{10–90\%}$ 0.51 ± 0.06, 0.76 ± 0.14, 0.63 ± 0.11, 0.26 ± 0.04; $t_{90–10\%}$ 0.87 ± 0.11, 1.27 ± 0.26, 2.04 ± 0.34, 0.51 ± 0.11; $\Delta P_o/P_{min}$ 85 ± 14 %, 109 ± 37 %, 61 ± 9 %, 49 ± 8 %. A Mann-Whitney *U* test was performed to test for significant differences between control conditions and hypoxia, low $[K^+]_o$ or ouabain. * Significant changes ($P < 0.05$). Interpretations of parameter values are discussed in the text.

mean open probability increased synchronously with these changes of neuronal activity.

Effect of the Na^+–K^+ pump blocker ouabain

The close correlation between burst discharges and P_o fluctuations indicates that P_o fluctuations originate from periodic variations of ATP consumption due to activation of the Na^+–K^+ pump. We therefore determined the changes in P_o shortly after application of the Na^+–K^+-ATPase blocker ouabain (20–100 μM). As previously described (Brockhaus *et al.* 1993), application of ouabain causes a slow blockade of the respiratory rhythm, as shown in Fig. 8*A* (insets). Analysis in 6/7 cells revealed a significant decline of P_o measured during and between respiratory bursts (Fig. 8*A*). For comparison of respiratory P_o fluctuations before and after ouabain application, typically less than 100 sweeps were available as the respiratory activity declined progressively. We found that the amplitudes of P_o fluctuations, $\Delta P_{peak}/P_{min}$, declined to 49 ± 8% (7 cells), as shown in the lowest panel of Fig. 8*B*. Ouabain also resulted in an increase in respiratory frequency and P_o peaks as shown by the decrease of the parameters $t_{10–90\%}$ and $t_{90–10\%}$ (Fig. 4*B*).

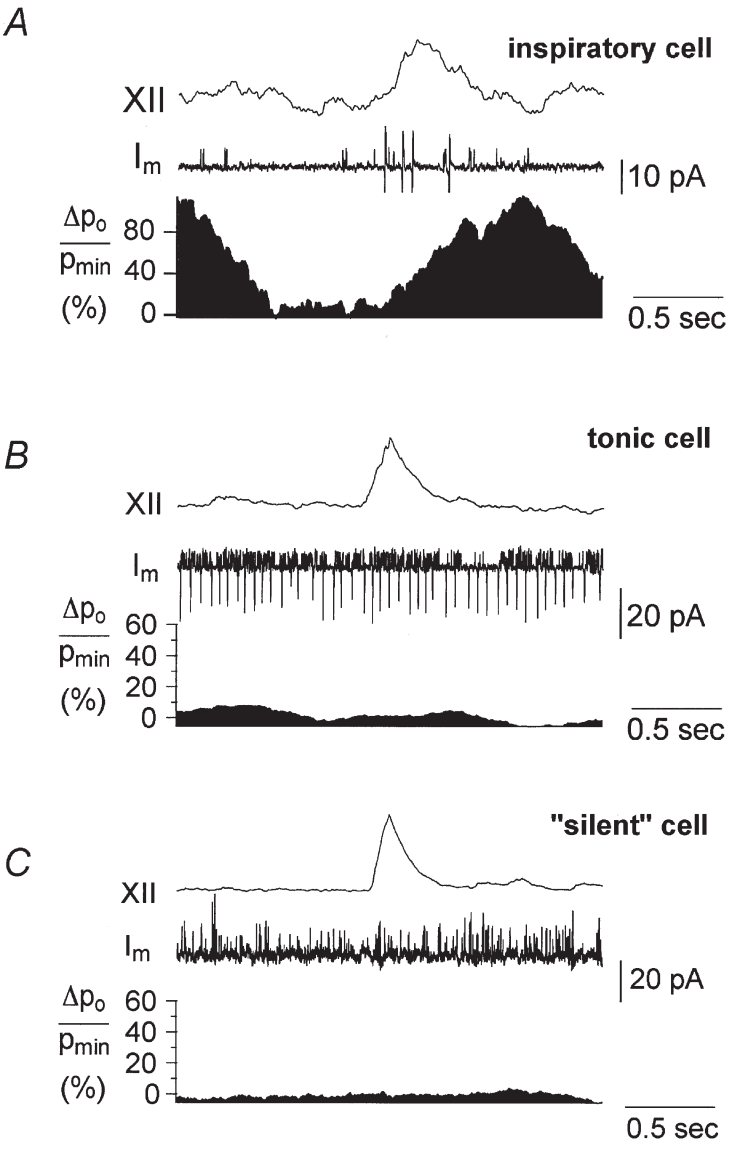

Figure 5. Control experiments

For controls, cell-attached recordings from tonic cells (2 cells) and 'silent' cells without action potential discharge (2 cells) were used (*B* and *C*, respectively). The analysis was performed as described for Fig. 3. A direct comparison of P_o fluctuations is difficult because of large differences in open probabilities. Thus P_o was not compared directly, but rather in terms of the relative change of P_o, $\Delta P_o/P_{min}$, expressed in %. It can be seen that neither the cell in *B* nor that in *C* displayed the same pattern of channel modulation as a control inspiratory neuron (*A*). Also, amplitudes of fluctuations of P_o were much lower than those observed in *A*.

DISCUSSION

We showed that medullary inspiratory neurons of the NMRI mouse express K_{ATP} channels composed of Kir6.2 and SUR1 subunits. This corresponds with the channel population typically found in pancreatic β-cells (Inagaki *et al.* 1995) and in neurons of the dorsal nucleus of the vagus nerve of the rat (Karschin *et al.* 1998).

K_{ATP} channels were revealed to be active even during normoxia and to contribute to the modulation of synaptic drives and hypoglossal rhythmic activity. Analysis of K_{ATP} channels in inspiratory neurons showed that P_o fluctuates in synchrony with rhythmic bursting of respiratory neurons. The functional aspect is that K_{ATP} channels are activity regulated and contribute to the modulation of ongoing spontaneous activity.

For quantitative description of such activity-dependent control, it is important to mention that the technique for calculating P_o fluctuations produced an unavoidable systematic error. Firstly, P_o could not be accurately computed during action potential discharges (APs). APs had to be subtracted from the trace and therefore some channel openings occurring during such APs and their afterpotentials have been missed. Consequently, P_o was underestimated during these discharge periods, i.e. in reality, peak P_o values are probably larger than described

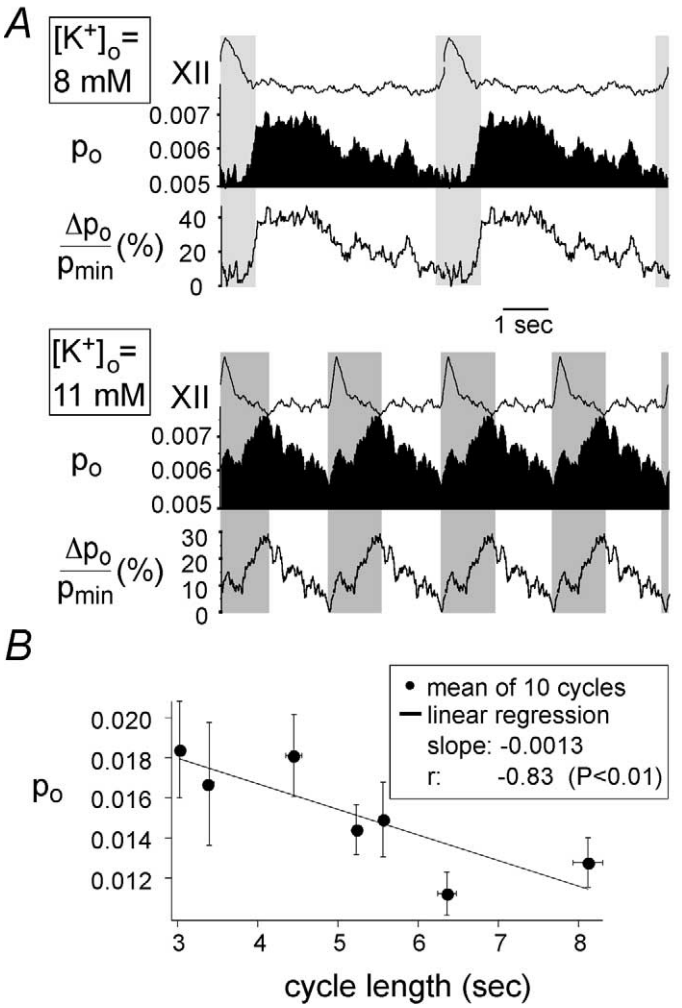

Figure 6. Changes in cycle lengths as induced by $[K^+]_o$ variation

A, fluctuations of P_o and $\Delta P_o/P_{min}$ for 8 mM (upper panel) or 11 mM $[K^+]_o$ (lower panel). One hundred traces of duration 5 s and 2.5 s were selected for a $[K^+]_o$ of 8 mM and 11 mM, respectively, and analysed as described in the text. Hypoglossal rootlet activity (XII), P_o and $\Delta P_o/P_{min}$ were reproduced and repeated twice (above) or four times (below) for better visualization of periodic activities. It can be seen that the cycle length decreases and the mean open probability increases as $[K^+]_o$ is elevated. However, the basic pattern of fluctuation remains the same: P_o rises during the inspiratory bursts and falls after the inspiratory burst. Changes in fluctuation parameters t_{delay}, T_{tot}, $t_{10-90\%}$, $t_{90-10\%}$ and $\Delta P_{peak}/P_{min}$ are discussed in the text. *B*, plot of mean P_o against cycle length. Mean values (± S.E.M.) of 10 cycles of similar lengths are represented by filled circles; the linear regression is given by a straight line (slope = −0.0013). Correlation analysis gave a correlation coefficient of −0.83 ($P < 0.01$).

here. Secondly, the durations of spontaneous respiratory cycles were never constant. For computation of P_o, however, many sweeps of variable cycle lengths had to be averaged. Consequently, estimates of respiration-related P_o changes were less accurate the further the P_o measurements were apart from the peak of the respiratory bursts, which was used to trigger the averages. This can be seen in Fig. 3*C* and *D*, where the selected time window preceded or respectively followed a respiratory burst. Thirdly, the membrane depolarization originating from the synaptic drive might lead to minor changes in single-channel currents and might thus affect P_o. It is unlikely, however, that the observed P_o fluctuations reflect such oscillations in membrane potential, as there was a clear time delay between the P_o minimum and peak membrane depolarization during the synaptic drive (Fig. 3*B*). At the time of minimal P_o, the cell had returned to its resting level. The contribution of voltage-dependent changes in P_o, therefore, appears to be negligible.

In contrast to pancreatic β-cells and cardiomyocytes, where variation of K_{ATP} channel openings originates from oscillations in the glycolytic pathway, our data in inspiratory neurons suggest a novel regulatory mechanism. Our findings clearly reveal activity-correlated K_{ATP} channel fluctuations, which probably originate from oscillations of ATP/ADP concentration ratios generated by periodic ATP consumption of Na^+–K^+-ATPase activity. This assumption follows the rationale that intracellular $[Na^+]$ accumulates during each respiratory burst of discharges, resulting in a periodic acceleration of Na^+–K^+ pumping. Such variations in Na^+–K^+-ATPase activity would lead to periodic fluctuations in submembrane $[ATP]_i$, directly inducing oscillations in P_o of local K_{ATP} channels. This hypothesis is consistent with the observed reduction of P_o oscillations after ouabain-induced blockade of Na^+–K^+-ATPase activity. Similar to other reports (Urbach *et al.* 1996; Kabakov, 1998; Abe *et al.* 1999), where coupling between K_{ATP} channels and Na^+–K^+ pumping was attributed to changes in the

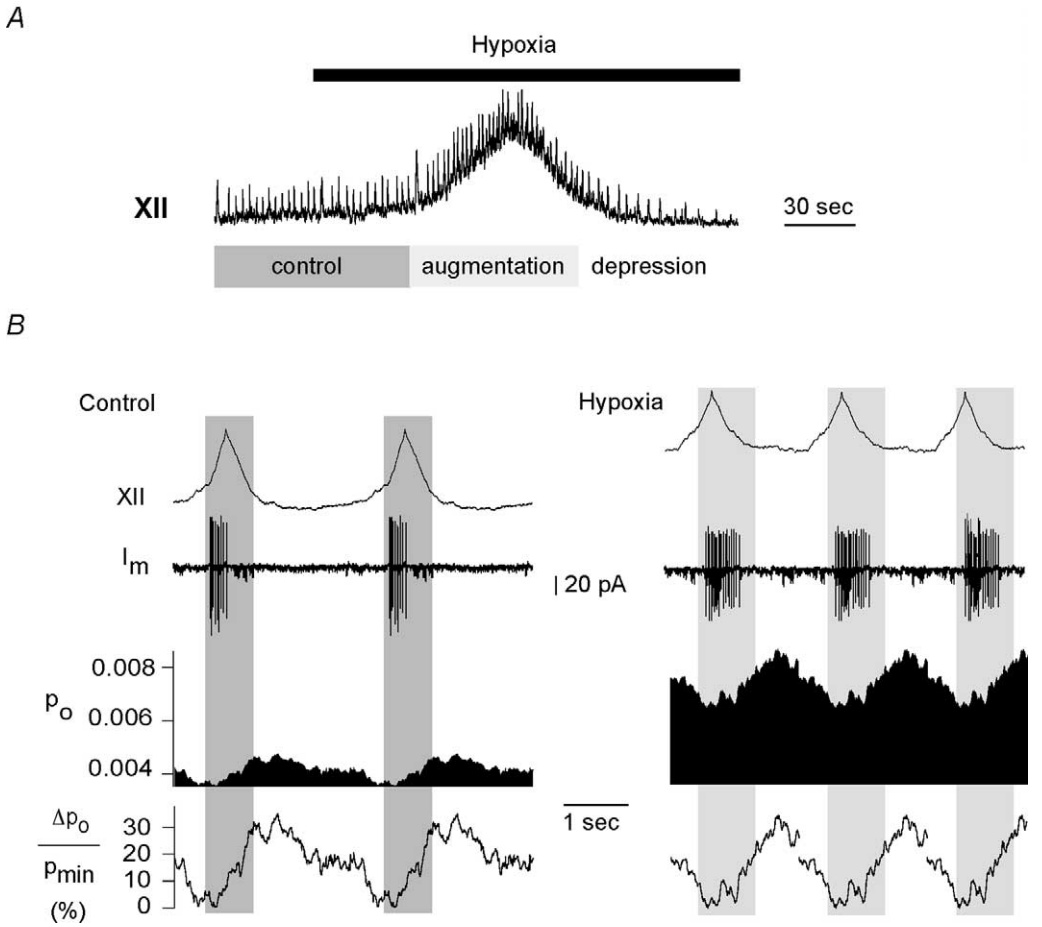

Figure 7. Changes in cycle length induced by hypoxia

A, the response of hypoglossal activity to hypoxia. P_o and $\Delta P_o/P_{min}$ were analysed separately for control sweeps (dark grey area) and for the augmentation phase of hypoxia (light grey area). Traces were reproduced twice during control (*B*, left panel, $n = 34$) and three times during hypoxia (*B*, right panel, $n = 21$). The open probability shows a marked increase during hypoxia (8 cells). The effect on fluctuation parameters is discussed in the text (see Fig. 4*B*).

ATP/ADP ratio, we observed a steady decline of K_{ATP} channel activity after ouabain application. Two separate mechanisms may contribute to this effect. Firstly, blockade of the Na^+–K^+-ATPase will lead to a reduction in ATP consumption leading to elevation of intracellular ATP concentrations and ATP/ADP ratios, and thus to a decline of K_{ATP} channel activity. Secondly, ouabain slowly depolarizes neurons (Cousin *et al.* 1995; Balestrino *et al.* 1999) and finally blocks AP discharges, resulting in a decreased Na^+ influx and lowered Na^+–K^+ pumping.

For a quantitative description of P_o fluctuations, $t_{10–90\%}$, $t_{90–10\%}$, $\Delta P_{peak}/P_{min}$ and T_{tot} were analysed. These parameters reflected a close similarity between P_o fluctuations and respiratory parameters, such as cycle frequency and burst durations. Manipulations of neuronal excitability induced by changes in $[K^+]_o$, ouabain or hypoxia led to alterations of these P_o parameters, which paralleled all changes in respiratory cycle length and cellular bursting behaviour: when respiratory frequency was lowered during reduction of $[K^+]_o$, T_{tot} and $t_{90–10\%}$ were prolonged. The surprising increase in 'decay time', $t_{90–10\%}$, indicates that ATP depletion starts with the onset of neuronal activity and accumulates during prolonged respiratory bursts, while ATP replenishment recovers slowly thereafter. This reveals that full ATP replenishment may take longer than the duration of interburst intervals. Enhancement of $t_{10–90\%}$ during hypoxia, which reflects a prolonged rise time of P_o, can be attributed to an increasing number of APs discharged per burst and consequently a stronger depletion of ATP. After ouabain application, the number and amplitude of APs were reduced, leading to a shorter delay of P_o maximum and accordingly a significant decrease in $t_{10–90\%}$ and $t_{90–10\%}$.

For all experimental conditions, the delay between onset of inspiratory burst activity and rise of P_o amounted to approximately 100 ms. Much faster activation rates were reported for the activation of the Na^+–K^+-ATPase (Munakata *et al.* 1998). Therefore, the longer delays in K_{ATP} channel reactivity seen in the present experiments seem to originate from other processes, for example from the voltage-clamp technique. We speculate that the propagation of action potentials to the membrane patch, where K_{ATP} channels were analysed, was probably blocked due to the forced holding potential of approximately −100 mV (pipette potential: +40 mV). Such lack of local Na^+ fluxes might provoke decreased ATP consumption. Secondly, the membrane patch that is sealed with the patch electrode probably forms an

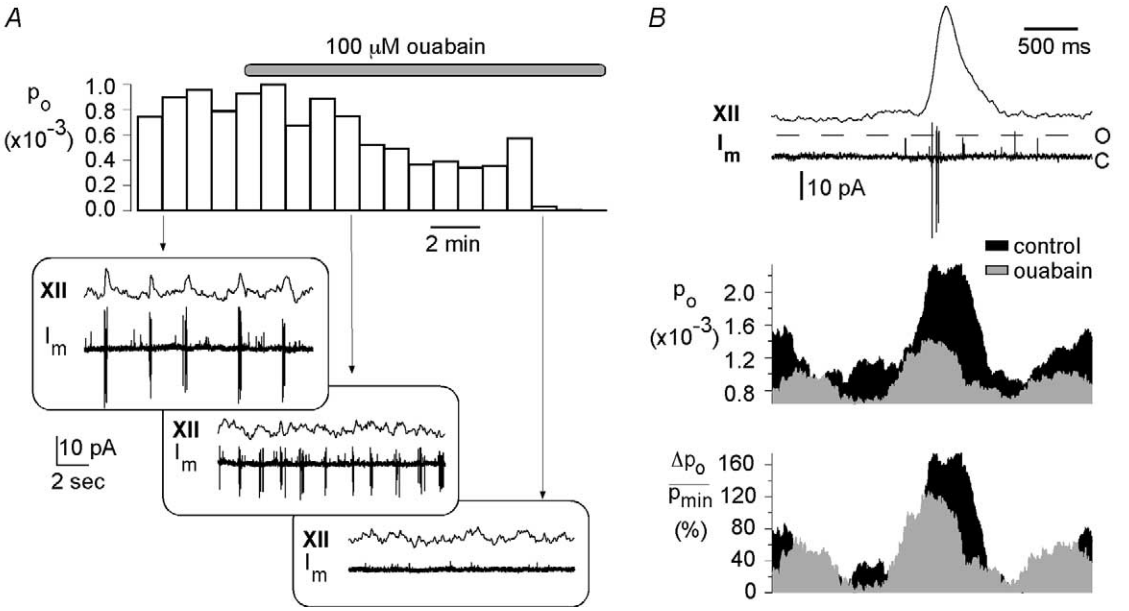

Figure 8. Effect of ouabain on P_o fluctuations

A, after application of 100 μM ouabain, P_o decreased from $0.88 \pm 0.10 \times 10^{-3}$ to $0.21 \pm 0.22 \times 10^{-3}$ (mean ± S.D.). Depicted are P_o values derived from consecutive data traces of 60 s duration. The boxes below show hypoglossal activity (XII) and membrane current (I_m) recorded at different phases of ouabain application. They clearly illustrate that the amplitudes of both respiratory rhythm and action potentials decrease until they are blocked completely approximately 7 min after ouabain application. A 3 s time window surrounding the inspiratory burst is shown in *B*. The two upper curves display sample traces of hypoglossal recordings (XII) and membrane current, I_m. Mean P_o curves were obtained by averaging over 100 traces (control) and 90 traces (ouabain) containing an inspiratory burst. The relative change in P_o, $\Delta P_o/P_{min}$, is depicted below.

omega-shape of variable dimension (Hamill *et al.* 1981), thus creating an artificial compartment that is functionally separated from the remainding cytosol and cell metabolism. We conclude that low local Na^+–K^+-ATPase activity and sustained ATP concentrations in the pipette-attached membrane patch explain a slower reactivity of partially isolated K_{ATP} channels. The high variability of delays measured in individual neurons might also reflect such differences in diffusion distances of ATP molecules from the patch membrane carrying the K_{ATP} channels to the electrically activated peri-patch membrane segments.

Assuming that a change in ATP concentration is a dominant factor for inducing fluctuations in K_{ATP} channel activity, P_o can be used to get a rough estimation of the changes in local free $[ATP]_i$. For such estimation we used the equation $[ATP] = K_d/(1/P_o^{1/4} - 1)$, postulating four ATP-binding sites with equal affinity as described by Ashcroft & Gribble (1998) and blockade of channels, when one of these binding sites is occupied. We assumed a K_d value of 29 μM (Ashcroft & Gribble, 1998). Figure 3*D* illustrates the temporal fluctuations of estimated $[ATP]_i$ values as well as changes in the ADP concentration derived from $[ATP]_i$. For all thirteen neurons analysed, such calculations indicate periodic changes in free $[ATP]_i$ ranging in the order of 5–40 μM. However, it should be emphasized that factors other than ATP, most noticeably ADP and pH, might contribute to the activation of P_o (Cason *et al.* 1995; Hilgemann, 1997; Hiraoka, 1997; Aguilar-Bryan & Bryan, 1999; Baukrowitz & Fakler, 2000). Indeed, the intracellular pH falls periodically by up to 0.2 pH units during periods of synaptic inhibition that follow respiratory bursts. The pH fluctuations originate from a HCO_3^- efflux through transmitter-regulated Cl^- channels (Ballanyi *et al.* 1994). Inhibition-dependent pH fluctuations could thus contribute to the activity- and ATP-induced P_o fluctuations. The conclusion is that estimated fluctuations of ATP concentrations derived from P_o variations were probably underestimated.

In conclusion, our results indicate that K_{ATP} channels are natural sensors of the instantaneous demand of metabolic energy. Their functional task appears to be a permanent and fast-acting adjustment of neuronal activity and cell metabolism. Therefore, K_{ATP} channels are endogenous regulators that damp rhythmic activity of neurons and contribute to membrane repolarization during and after each burst of action potentials. We conclude that functional neuronal networks demand a continuous $[ATP]_i$ supply and fast replenishment, and use K_{ATP} channels to accurately adjust the excitability of neurons to stabilize their activity levels and to protect network integrity.

Abe, T., Sato, T., Kiyosue, T., Saikawa, T., Sakata, T. & Arita, M. (1999). Inhibition of Na^+–K^+ pump alleviates the shortening of action potential duration caused by metabolic inhibition via blockade of K_{ATP} channels in coronary perfused ventricular muscles of guinea-pigs. *Journal of Molecular and Cellular Cardiology* **31**, 533–542.

Aguilar-Bryan, L. & Bryan, J. (1999). Molecular biology of adenosine triphosphate-sensitive potassium channels. *Endocrine Reviews* **20**, 101–135.

Aguilar-Bryan, L., Nichols, C. G., Wechsler, S. W., Clement, J. P. T., Boyd, A. E. III, Gonzalez, G., Herrera-Sosa, H., Nguy, K., Bryan, J. & Nelson, D. A. (1995). Cloning of the β cell high-affinity sulfonylurea receptor: a regulator of insulin secretion. *Science* **268**, 423–426.

Ashcroft, F. M. & Gribble, F. M. (1998). Correlating structure and function in ATP-sensitive K^+ channels. *Trends in Neurosciences* **21**, 288–294.

Balestrino, M., Young, J. & Aitken, P. (1999). Block of (Na^+,K^+)ATPase with ouabain induces spreading depression-like depolarization in hippocampal slices. *Brain Research* **838**, 37–44.

Ballanyi, K., Doutheil, J. & Brockhaus, J. (1996). Membrane potentials and microenvironment of rat dorsal vagal cells *in vitro* during energy depletion. *Journal of Physiology* **495**, 769–784.

Ballanyi, K., Muckenhoff, K., Bellingham, M. C., Okada, Y., Scheid, P. & Richter, D. W. (1994). Activity-related pH changes in respiratory neurones and glial cells of cats. *NeuroReport* **6**, 33–36.

Baukrowitz, T. & Fakler, B. (2000). K_{ATP} channels gated by intracellular nucleotides and phospholipids. *European Journal of Biochemistry* **267**, 5842–5848.

Brockhaus, J., Ballanyi, K., Smith, J. C. & Richter, D. W. (1993). Microenvironment of respiratory neurons in the *in vitro* brainstem–spinal cord of neonatal rats. *Journal of Physiology* **462**, 421–445.

Cason, B. A., Gordon, H. J., Avery, E. G. T. & Hickey, R. F. (1995). The role of ATP sensitive potassium channels in myocardial protection. *Journal of Cardiac Surgery* **10**, 441–444.

Cousin, M. A., Nicholls, D. G. & Pocock, J. M. (1995). Modulation of ion gradients and glutamate release in cultured cerebellar granule cells by ouabain. *Journal of Neurochemistry* **64**, 2097–2104.

Eberwine, J., Yeh, H., Miyashiro, K., Cao, Y., Nair, S., Finnell, R., Zettel, M. & Coleman, P. (1992). Analysis of gene expression in single live neurons. *Proceedings of the National Academy of Sciences of the USA* **89**, 3010–3014.

Haddad, G. G. & Donnelly, D. F. (1990). O_2 deprivation induces a major depolarization in brainstem neurons in the adult but not in the neonatal rat. *Journal of Physiology* **429**, 411–428.

Hamill, O. P., Marty, A., Neher, E., Sakmann, B. & Sigworth, F. J. (1981). Improved patch-clamp techniques for high-resolution current recording from cells and cell-free membrane patches. *Pflügers Archiv* **391**, 85–100.

Hilgemann, D. W. (1997). Cytoplasmic ATP-dependent regulation of ion transporters and channels: mechanisms and messengers. *Annual Review of Physiology* **59**, 193–220.

Hiraoka, M. (1997). Pathophysiological functions of ATP-sensitive K^+ channels in myocardial ischemia. *Japanese Heart Journal* **38**, 297–315.

Inagaki, N., Gonoi, T., Clement, J. P. T., Namba, N., Inazawa, J., Gonzalez, G., Aguilar-Bryan, L., Seino, S. & Bryan, J. (1995). Reconstitution of IKATP: an inward rectifier subunit plus the sulfonylurea receptor. *Science* **270**, 1166–1170.

Isomoto, S., Kondo, C., Yamada, M., Matsumoto, S., Higashiguchi, O., Horio, Y., Matsuzawa, Y. & Kurachi, Y. (1996). A novel sulfonylurea receptor forms with BIR (Kir6.2) a smooth muscle type ATP-sensitive K^+ channel. *Journal of Biological Chemistry* **271**, 24321–24324.

Jiang, C. & Haddad, G. G. (1997). Modulation of K^+ channels by intracellular ATP in human neocortical neurons. *Journal of Neurophysiology* **77**, 93–102.

Kabakov, A. Y. (1998). Activation of K_{ATP} channels by Na/K pump in isolated cardiac myocytes and giant membrane patches. *Biophysical Journal* **75**, 2858–2867.

Karschin, A., Brockhaus, J. & Ballanyi, K. (1998). K_{ATP} channel formation by the sulphonylurea receptors SUR1 with Kir6.2 subunits in rat dorsal vagal neurons *in situ*. *Journal of Physiology* **509**, 339–346.

Kinard, T. A., de Vries, G., Sherman, A. & Satin, L. S. (1999). Modulation of the bursting properties of single mouse pancreatic β-cells by artificial conductances. *Biophysical Journal* **76**, 1423–1435.

Larsson, O., Kindmark, H., Brandstrom, R., Fredholm, B. & Berggren, P. O. (1996). Oscillations in K_{ATP} channel activity promote oscillations in cytoplasmic free Ca^{2+} concentration in the pancreatic β cell. *Proceedings of the National Academy of Sciences of the USA* **93**, 5161–5165.

Lynch, J. W. & Barry, P. H. (1989). Action potentials initiated by single channels opening in a small neuron (rat olfactory receptor). *Biophysical Journal* **55**, 755–768.

Miki, T., Nagashima, K., Tashiro, F., Kotake, K., Yoshitomi, H., Tamamoto, A., Gonoi, T., Iwanaga, T., Miyazaki, J. & Seino, S. (1998). Defective insulin secretion and enhanced insulin action in K_{ATP} channel-deficient mice. *Proceedings of the National Academy of Sciences of the USA* **95**, 10402–10406.

Mironov, S. L., Langohr, K., Haller, M. & Richter, D. W. (1998). Hypoxia activates ATP-dependent potassium channels in inspiratory neurones of neonatal mice. *Journal of Physiology* **509**, 755–766.

Munakata, M., Fujimoto, M., Jin, Y. H. & Akaike, N. (1998). Characterization of electrogenic Na/K pump in rat neostriatal neurons. *Brain Research* **800**, 282–293.

O'Rourke, B., Ramza, B. M. & Marban, E. (1994). Oscillations of membrane current and excitability driven by metabolic oscillations in heart cells. *Science* **265**, 962–966.

Pierrefiche, O., Bischoff, A. M. & Richter, D. W. (1996). ATP-sensitive K^+ channels are functional in expiratory neurones of normoxic cats. *Journal of Physiology* **494**, 399–409.

Prentki, M., Tornheim, K. & Corkey, B. E. (1997). Signal transduction mechanisms in nutrient-induced insulin secretion. *Diabetologia* **40**, suppl. 2, S32–41.

Rajendra, S., Lynch, J. W. & Barry, P. H. (1992). An analysis of Na^+ currents in rat olfactory receptor neurons. *Pflügers Archiv* **420**, 342–346.

Sakura, H., Ammala, C., Smith, P. A., Gribble, F. M. & Ashcroft, F. M. (1995). Cloning and functional expression of the cDNA encoding a novel ATP- sensitive potassium channel subunit expressed in pancreatic β-cells, brain, heart and skeletal muscle. *FEBS Letters* **377**, 338–344.

Smith, J. C., Ellenberger, H. H., Ballanyi, K., Richter, D. W. & Feldman, J. L. (1991). Pre-Botzinger complex: a brainstem region that may generate respiratory rhythm in mammals. *Science* **254**, 726–729.

Terzic, A., Jahangir, A. & Kurachi, Y. (1995). Cardiac ATP-sensitive K^+ channels: regulation by intracellular nucleotides and K^+ channel-opening drugs. *American Journal of Physiology* **269**, C525–545.

Urbach, V., Van Kerkhove, E., Maguire, D. & Harvey, B. J. (1996). Cross-talk between ATP-regulated K^+ channels and Na^+ transport via cellular metabolism in frog skin principal cells. *Journal of Physiology* **491**, 99–109.

Yamada, M., Isomoto, S., Matsumoto, S., Kondo, C., Shindo, T., Horio, Y. & Kurachi, Y. (1997). Sulphonylurea receptor 2B and Kir6.1 form a sulphonylurea-sensitive but ATP-insensitive K^+ channel. *Journal of Physiology* **499**, 715–720.

Zawar, C., Plant, T. D., Schirra, C., Konnerth, A. & Neumcke, B. (1999). Cell-type specific expression of ATP-sensitive potassium channels in the rat hippocampus. *Journal of Physiology* **514**, 327–341.

Acknowledgements

This work was supported by the DFG. We thank Nicole Hartelt for excellent technical assistance.

Corresponding author

M. Haller: Physiologisches Institut, Georg August-Universität Göttingen, Humboldtallee 23, D-37073 Göttingen, Germany.

Email: mirjam@neuro-physiol.med.uni-goettingen.de